

Article

Wilsonian Effective Action and Entanglement Entropy

Satoshi Iso ^{1,2,*}, Takato Mori ^{1,2,*}  and Katsuta Sakai ^{1,*} 

¹ KEK Theory Center, High Energy Accelerator Research Organization (KEK), Oho 1-1, Tsukuba 305-0801, Ibaraki, Japan

² Department of Particle and Nuclear Physics, School of High Energy Accelerator Science, The Graduate University for Advanced Studies (SOKENDAI), Oho 1-1, Tsukuba 305-0801, Ibaraki, Japan

* Correspondence: satoshi.iso@kek.jp (S.I.); moritaka@post.kek.jp (T.M.); sakaika@post.kek.jp (K.S.)

Abstract: This is a continuation of our previous works on entanglement entropy (EE) in interacting field theories. In previous papers, we have proposed the notion of \mathbb{Z}_M gauge theory on Feynman diagrams to calculate EE in quantum field theories and shown that EE consists of two particular contributions from propagators and vertices. We have also shown that the purely non-Gaussian contributions from interaction vertices can be interpreted as renormalized correlation functions of composite operators. In this paper, we will first provide a unified matrix form of EE containing both contributions from propagators and (classical) vertices, and then extract further non-Gaussian contributions based on the framework of the Wilsonian renormalization group. It is conjectured that the EE in the infrared is given by a sum of all the vertex contributions in the Wilsonian effective action.

Keywords: entanglement entropy; interacting quantum field theory; Wilsonian effective action



Citation: Iso, S.; Mori, T.; Sakai, K. Wilsonian Effective Action and Entanglement Entropy. *Symmetry* **2021**, *13*, 1221. <https://doi.org/10.3390/sym13071221>

Academic Editor: Loriano Bonora

Received: 31 May 2021

Accepted: 1 July 2021

Published: 7 July 2021

Publisher's Note: MDPI stays neutral with regard to jurisdictional claims in published maps and institutional affiliations.



Copyright: © 2021 by the authors. Licensee MDPI, Basel, Switzerland. This article is an open access article distributed under the terms and conditions of the Creative Commons Attribution (CC BY) license (<https://creativecommons.org/licenses/by/4.0/>).

1. Introduction

Entanglement entropy (EE) captures correlations for bipartite entangled states between two subspaces, in particular spatially separated regions, and has been widely investigated in conformal field theories (CFTs) [1–5], perturbations from CFTs [6–8] or in the context of AdS/CFT correspondence [9–12] (for review, [12,13]). In free quantum field theories (QFTs), where the vacuum wavefunctional is Gaussian, EE is well-understood [1,14] and we can perform explicit calculations [15–19]. On the other hand, we have little understanding of EE in general interacting QFTs, apart from exactly solvable cases [20] or some supersymmetric theories [12,13,21–23]. EE in interacting theories are discussed in perturbative [24,25], nonperturbative [26–32], lattice [33–37], or in terms of variational trial wave functions [28–30].

In interacting QFTs, EE is divergent and needs regularizations. First, EE is UV divergent because there are infinitely many degrees of freedom. This divergence occurs even in a free theory. Second, in interacting theories, the infinite degrees of freedom cause UV divergences in physical parameters and renormalizations are necessary to extract finite results. Finally, if a theory contains massless fields, it may cause IR divergence, but in this paper, we consider a massive theory so that the IR divergences are assumed to be absent.

The EE in the infrared limit, or its variation with respect to some parameters such as mass or coupling constants, is determined by correlations of the renormalized vacuum wave function and should be independent of the UV cutoff. In this sense, the IR part of EE must be determined by the IR fixed point of the renormalization group (RG). On the other hand, EE at a fixed scale will change along the RG flow on which a theory transmutes from one fixed point to another. In order to understand these behaviors of EE, the Wilsonian approach of renormalization [38–41] will be useful. The Wilsonian effective action (EA) describes a flow of effective actions at a given scale where all higher momentum fluctuations of fields are integrated out, together with rescaling of the momentum so as to make the UV cutoff back to the original one.

In this paper, we will investigate EE in interacting field theories based on the Wilsonian picture of renormalization combined with our previous works [42,43] based on the \mathbb{Z}_M gauge theory on Feynman diagrams. In [42], we succeeded to extract two particular contributions to EE in interacting field theories: one is the Gaussian contributions written in terms of renormalized two-point correlation functions in the two-particle irreducible (2PI) formalism. Another set of important contributions comes from *classical* vertices, which reflects non-Gaussianity of the vacuum wave function. In [43], we showed that the vertex contributions can be interpreted as contributions from renormalized two-point correlation functions of *composite operators*. These results are obtained by evaluating EE in the notion of the \mathbb{Z}_M gauge theory on Feynman diagrams, whose picture is derived from the replica method of EE (the number of replicas n is replaced by $n = 1/M$). In the formulation, EE is given by a sum of various configurations of \mathbb{Z}_M fluxes on plaquettes in Feynman diagrams and the above two contributions to EE are described by two particular types of flux configurations. Thus, an important question left unanswered is how to extract other contributions described by other configurations of fluxes. In this paper, we address this question in the framework of the Wilsonian RG, where a variety of *quantum* vertices appears as the energy scale decreases.

For this purpose, we first generalize our previous results to describe operator mixings. We also give a natural, unified description of the contributions to EE from propagators and vertices in a matrix form. This unified description is one of the main results of the present paper. By using this generalized expression of EE, we conjecture that the IR part of EE is given by a sum of the propagator and vertex contributions in the Wilsonian EA.

The paper is organized as follows: in Section 2, we first briefly summarize the notion of the \mathbb{Z}_M gauge theory on Feynman diagrams, two particular contributions to EE from propagators and vertices in the ϕ^4 scalar theory, and an interpretation of the vertex contribution in terms of a correlator of a composite operator. In addition, we give a unified description of both contributions in a matrix form. In Section 3, we generalize it when various operators are mixed with each other and also when the composite operators have spins in the two-dimensional spacetime normal to the boundary. In Section 4, we discuss the IR behavior of EE in the framework of the Wilsonian RG and give a conjecture that EE in the IR is given by a sum of the propagator and vertex contributions in the Wilsonian EA. Finally, we give conclusions in Section 5. In Appendix A, we prove the area law for Rényi entropy and the capacity of entanglement [44,45]. In Appendix B, we give a proof that all the single twist contributions from vertices are written in the 1-loop type expression of composite operators. This is a generalization of the proof for the propagator contributions based on the 2PI formalism.

2. Summary of Previous Works

In this section, we first summarize our previous works in [42,43], and then introduce a new concept of the *generalized* 1PI in order to unify the contributions to EE from propagators and vertices.

2.1. \mathbb{Z}_M Gauge Theory on Feynman Diagrams

Entanglement entropy of a subsystem A is defined by

$$S_{EE} = -\text{Tr}_A \rho_A \log \rho_A, \quad (1)$$

where $\rho_A = \text{Tr}_{\bar{A}} \rho_{\text{tot}}$ is a reduced density matrix of ρ_{tot} obtained by integrating out the complementary system \bar{A} in the Hilbert space. In this paper, we take A as a half space on a time slice in a $(d+1)$ -dimensional spacetime and utilize the orbifold method [46,47] to calculate S_{EE} . This method is a variation of the replica trick for EE in which EE is given through the $n \rightarrow 1$ limit of Rényi entropy $S_n = \frac{1}{1-n} \log \text{Tr} \rho_A^n$ [1]; by taking the replica

parameter $n = 1/M$, we consider free energy of interacting quantum field theories on the orbifold $\mathbb{R}^2/\mathbb{Z}_M \times \mathbb{R}^{d-1}$ denoted by $F^{(M)}$. Then, EE is written as

$$S_{EE} = -\frac{\partial(MF^{(M)})}{\partial M}\Big|_{M \rightarrow 1}. \quad (2)$$

Since a physical state of the \mathbb{Z}_M orbifold theory is invariant under the \mathbb{Z}_M projection operator,

$$\hat{P} = \sum_{n=0}^{M-1} \frac{\hat{g}^n}{M}, \quad (3)$$

where \hat{g} is a $2\pi/M$ rotation operator around the origin, and the orbifold theory can be interpreted as the \mathbb{Z}_M gauge theory on Feynman diagrams. Namely, each propagator in a Feynman diagram is sandwiched by the projection operators; this corresponds to assigning a *twist* n_i on the i -th propagator $G(\hat{g}^{n_i}x, y)$ and summing over all independent configurations of such twists. Then, the notion of \mathbb{Z}_M gauge symmetry appears since we can rotate away some of the twists of propagators by the \mathbb{Z}_M gauge transformations on vertices of the Feynman diagram. As a result, we can classify independent configurations of twists up to \mathbb{Z}_M transformations in terms of \mathbb{Z}_M fluxes of twists on plaquettes. Here, a flux of twists on a plaquette is defined by a sum of twists around the plaquette as shown in Figure 1.

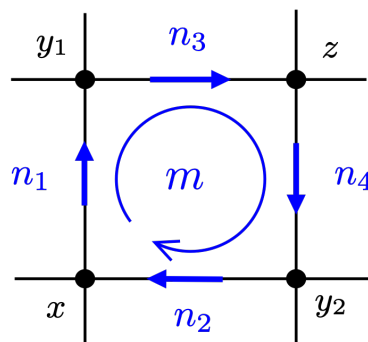


Figure 1. The figure shows a \mathbb{Z}_M twist configuration on a Feynman diagram. Given twists $\{n_i\}$ assigned on propagators, a flux of twists $m = 0, \dots, M-1$ is defined on a plaquette by a sum of twists around the plaquette $m = \sum_i n_i \bmod M$. The flux is invariant under \mathbb{Z}_M gauge transformations on vertices.

A simple example of the \mathbb{Z}_M invariant configuration is given by Figure 2. The 1-loop diagram has only one plaquette and the \mathbb{Z}_M invariant twist is given by the flux m . The number of independent flux is always 1 even if we divide the propagator into several connecting pieces. One may think that each propagator can be twisted separately, but such multiplicities are removed by the \mathbb{Z}_M transformations on vertices connecting the divided propagators. Thus, there is only one independent twist in the 1-loop diagram. This property is essential to prove our main result of Equation (32) and responsible for the fact that EE can be written as a sum of 1-loop type diagrams of various composite operators. See the proof in Appendix B. See also the discussions in Section 4B and Section 4C in our previous paper [43].

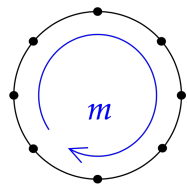


Figure 2. There is a single twist for a 1-loop diagram. The number of independent twists is unchanged even if we divide the propagator into multiple connecting pieces as drawn in the figure.

2.2. Propagator Contributions to EE

In order to evaluate EE in Equation (2), we need to extract all the configurations of fluxes that do not vanish in the $M \rightarrow 1$ limit. In the previous papers, we have shown that, if all the fluxes of twists are zero, they do not contribute to EE in Equation (2), which assures the area law of EE (It is easy to see that this property also holds for the Rényi entropy or entanglement capacity, and so does the area law. For more details, see Appendix A). Among various configurations contributing to EE, we have focused on two particular configurations.

The first type of configurations are given in Figure 3 and can be interpreted as a twist of the propagator. The simplest configuration of this type is given by Figure 2 and already present in a free field theory. Interactions induce renormalization of physical quantities, such as a mass, appearing in the EE. A seminal calculation was studied by Hertzberg [24] and completed in our previous papers based on the two-particle irreducible formalism (2PI) where we have shown that the propagator contributions are exactly given by

$$S_{\text{propagator}} = -\frac{V_{d-1}}{6} \int^{1/\epsilon} \frac{d^{d-1}k_{\parallel}}{2(2\pi)^{d-1}} \log[G^{-1}(\mathbf{0}; k_{\parallel})\epsilon^2] \quad (4)$$

$$= -\frac{V_{d-1}}{6} \int^{1/\epsilon} \frac{d^{d-1}k_{\parallel}}{2(2\pi)^{d-1}} \log[(G_0^{-1} - \Sigma)(\mathbf{0}; k_{\parallel})\epsilon^2], \quad (5)$$

where G is the renormalized propagator (The same symbol G is used to represent the Green function in coordinate and momentum spaces for notational simplicity. They are distinguished by their arguments if necessary.) and V_{d-1} is the volume of the boundary ∂A . The $(d+1)$ -dimensional momentum is written as (k, k_{\parallel}) , where k is the two-dimensional components of time and the direction normal to the boundary and k_{\parallel} is the $(d-1)$ -dimensional components parallel to the boundary. The UV cutoff ϵ is introduced. Writing the full inverse propagator as $G^{-1} = (G_0^{-1} - \Sigma)$, the logarithm can be expanded as a sum,

$$-\log G^{-1} = -\log G_0^{-1} + \sum_{n=1} \frac{(G_0 \Sigma)^n}{n}. \quad (6)$$

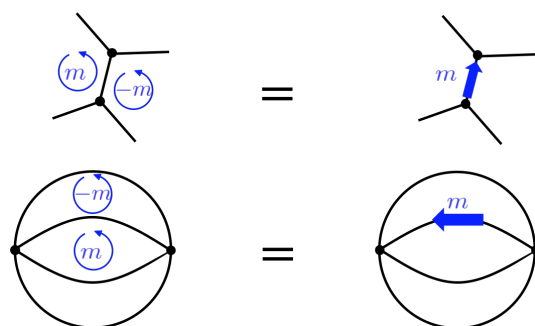


Figure 3. Twist of a propagator: if the fluxes of plaquettes straddling a shared propagator are given by m and $-m$, such a configuration is interpreted as a twist of the shared propagator. The upper figures show a relevant part in a general Feynman diagram that twists the propagator. The lower figures are an example of such a configuration in a 3-loop diagram.

Then, it can be interpreted as a chain of free propagators connected by the self-energy Σ . On the other hand, the full propagator G itself is expanded similarly but without the $1/n$ factor. This $1/n$ factor in the EE comes from the redundancy of twists: twisting n propagators in the chain is not independent. There is only a single twist in the plaquette as explained at the end of Section 2.1. If we twisted every propagator in the chain, it would over count the contributions to EE from the 1-loop Feynman diagram.

2.3. Vertex Contributions to EE and Generalized 1PI

The second type of configurations of fluxes we are going to focus on is given by Figure 4 for the ϕ^4 scalar theory, $\mathcal{L}_{\text{pot}} = \lambda_4 \phi^4 / 4$. These configurations of fluxes are interpreted as twists of the interaction vertices, which, in turn, are regarded as twists of the corresponding composite operators. This interpretation is obtained by opening a 4-point vertex into two 3-point vertices and assign the twist to the propagator connecting the two 3-point vertices. Corresponding to three different channels of the opening, s , t , and u , there are three different configurations of fluxes and contributions to EE, respectively. If different quantum numbers are assigned to these three channels, we can utilize a method of auxiliary fields and EE is given by a *sum* of propagator contributions of three different auxiliary fields as shown in [43]. If composite operators propagating three channels are mixed like the ϕ^4 -theory, we cannot use the method of auxiliary fields, but from diagrammatic analysis (see Appendix B), we can show that it is written in terms of a correlation function of composite operators. In the case of the ϕ^4 -theory, it is given [43] by

$$S_{\text{vertex}} = \frac{V_{d-1}}{6} \int^{1/\epsilon} \frac{d^{d-1} k_{\parallel}}{2(2\pi)^{d-1}} \log \left[1 - \frac{3}{2} \lambda_4 G_{\phi^2 \phi^2}(\mathbf{0}, k_{\parallel}) \right], \quad (7)$$

where

$$G_{\phi^2 \phi^2}(x - y) := \langle [\phi^2](x) [\phi^2](y) \rangle. \quad (8)$$

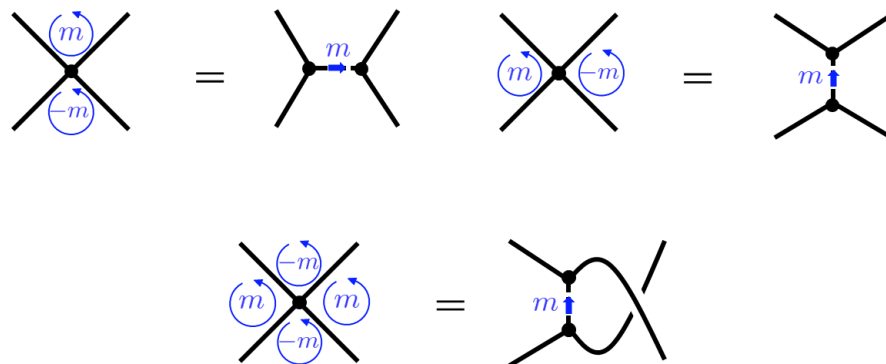


Figure 4. Twist of a vertex: three types of configurations can be attributed to a twist of the vertex. The dotted lines in the figures on the right-hand sides represent a virtual propagator that appears by opening the four-point vertex into a pair of three-point vertices by a delta function. The twist of a vertex is interpreted as a twist of the dotted propagator.

In the following, the cutoff ϵ is not explicitly written for notational simplicity, as it can be recovered by dimensional analysis. The square brackets $[\mathcal{O}]$ represent the normal ordering of an operator \mathcal{O} . The coefficient $-3\lambda_4/2$ is a product of $-\lambda_4/4$ and 6, where $-\lambda_4/4$ is the coefficient in front of the interaction vertex and the coefficient 6 is a combinatorial factor for separating four $\phi(x)$'s into a pair of $\phi^2(x)$ and $\phi^2(y)$. As shown in Figure 5, the Green function of the composite operator can be written as

$$G_{\phi^2 \phi^2} = \Sigma_{\phi^2 \phi^2}^{(g)} + \left(\frac{-3\lambda_4}{2} \right) (\Sigma_{\phi^2 \phi^2}^{(g)})^2 + \left(\frac{-3\lambda_4}{2} \right)^2 (\Sigma_{\phi^2 \phi^2}^{(g)})^3 + \dots$$

$$= \frac{\Sigma_{\phi^2\phi^2}^{(g)}}{1 - \left(\frac{-3\lambda_4}{2}\right)\Sigma_{\phi^2\phi^2}^{(g)}}, \quad (9)$$

where $\Sigma_{\phi^2\phi^2}^{(g)}$ is the 1PI self-energy of $[\phi^2]$ in a *generalized* sense. We call it g-1PI. Namely, the quantity with the superscript (g) does not contain a diagram like Figure 6 that is separable by cutting a vertex in the middle. We call such a diagram a beads diagram: 1PI in the ordinary sense but not in the generalized sense. Thus, these bead diagrams are not included in g-1PI diagrams.

$$G_{\phi^2\phi^2} = \text{Diagram } 1 + \text{Diagram } 2 + \text{Diagram } 3 + \dots$$

Figure 5. A Green function of a composite operator can be written in terms of the generalized self-energy $\Sigma_{\phi^2\phi^2}^{(g)}$, which is 1PI with respect to the propagator of the composite operator at the vertex as well as the fundamental field.

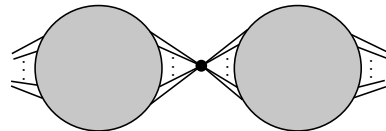


Figure 6. Beads diagram: this diagram is not 1PI in the *generalized* sense since it is separable by cutting the propagator at the opened vertex.

By using Equation (9), we can rewrite Equation (7) as

$$S_{\text{vertex}} = -\frac{V_{d-1}}{6} \int^{1/\epsilon} \frac{d^{d-1}k_{\parallel}}{2(2\pi)^{d-1}} \log \left[1 - \left(-\frac{3}{2}\lambda_4\right) \Sigma_{\phi^2\phi^2}^{(g)} \right]. \quad (10)$$

In the following equations including Equation (10), the argument ($k = 0, k_{\parallel}$) of the integrand for the k_{\parallel} integral is implicit. Now, we can write both the propagator and vertex contributions in Equations (5) and (10) in a unified matrix form as

$$S_{EE}^{(\phi^4)} = -\frac{V_{d-1}}{6} \int^{1/\epsilon} \frac{d^{d-1}k_{\parallel}}{2(2\pi)^{d-1}} \text{tr} \log \left[\hat{G}_0^{-1} - \hat{\lambda} \hat{\Sigma}^{(g)} \right], \quad (11)$$

where

$$\hat{G}_0 = \begin{pmatrix} G_0 & 0 \\ 0 & 1 \end{pmatrix}, \quad \hat{\lambda} = \begin{pmatrix} 1 & 0 \\ 0 & -3\lambda_4/2 \end{pmatrix}, \quad \hat{\Sigma}^{(g)} = \begin{pmatrix} \Sigma_{\phi^2\phi^2}^{(g)} & 0 \\ 0 & \Sigma_{\phi^2\phi^2}^{(g)} \end{pmatrix}. \quad (12)$$

In the following, we first generalize these results to include higher-point vertices whose composite operators are mixed in a complicated way. Then, we apply the concept of Wilsonian effective action to extract further contributions to the IR part of the EE. It is important to note that the form of Equation (11) is convenient for a unified description in the following discussions, but it is always possible to go back to the form like Equation (7), where the vertex contributions are written in terms of the ordinary renormalized propagators without the superscript (g) . In addition, note that all the single twist contributions from a vertex can be written in the above 1-loop type formula, Equation (7) or Equation (12). In the case of the propagator contributions to EE, we have proved the statement by using the 2PI formalism in [42,43]. Here, we use a diagrammatic method to prove it for the vertex contributions in Appendix B.

3. General Vertex Contributions to EE

In this section, we extend the analysis of vertex contributions to EE from the ϕ^4 interaction to more general cases.

3.1. ϕ^6 Scalar Field Theory

First, let us consider the ϕ^6 interaction,

$$\mathcal{L}_{\text{pot}} = \frac{\lambda_6}{6} \phi^6. \quad (13)$$

In this case, we have two types of vertex configurations (The ϕ^6 interaction will induce ϕ^4 interaction by contracting two ϕ 's, but, in this section, we simply set it zero by renormalization and do not consider contributions to EE from such diagrams as the vertex contributions at this stage. A model containing both ϕ^4 and ϕ^6 interaction vertices are studied in the next section.) as drawn in Figure 7, and three types of composite operators need to be introduced, ϕ^2 , ϕ^4 , and ϕ^3 , to extract all the vertex contributions to EE. Since the theory has \mathbb{Z}_2 invariance under $\phi \rightarrow -\phi$, the \mathbb{Z}_2 -even operators, ϕ^2 and ϕ^4 , are mixed with themselves while the \mathbb{Z}_2 -odd operator ϕ^3 is mixed with the fundamental field ϕ . Therefore, the propagator contribution in Equation (5) needs a modification.

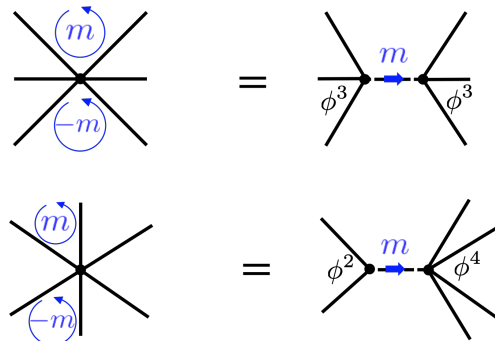


Figure 7. Two different composite operators appear by opening the ϕ^6 vertex. Each flux configuration corresponds to twisting the propagator of the respective composite operator.

First, let us consider the modified propagator contributions in the ϕ^6 theory. Such contributions come from 1-loop type diagrams of mixed correlations of ϕ and ϕ^3 operators. They are given by (Figure 8)

$$S_{\mathbb{Z}_2\text{-odd}} = -\frac{V_{d-1}}{6} \int \frac{d^{d-1}k_{\parallel}}{2(2\pi)^{d-1}} \text{tr} \log \left[\hat{G}_0^{-1} - \hat{\lambda} \hat{\Sigma}^{(g)} \right], \quad (14)$$

where

$$\hat{G}_0 = \begin{pmatrix} G_0 & 0 \\ 0 & 1 \end{pmatrix}, \quad \hat{\lambda} = \begin{pmatrix} 1 & 0 \\ 0 & -10\lambda_6/3 \end{pmatrix}, \quad \hat{\Sigma}^{(g)} = \begin{pmatrix} \Sigma^{(g)} & \Sigma_{\phi\phi^3}^{(g)} \\ \Sigma_{\phi^3\phi}^{(g)} & \Sigma_{\phi^3\phi^3}^{(g)} \end{pmatrix}. \quad (15)$$

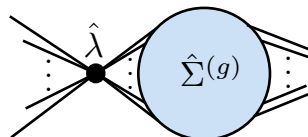


Figure 8. A Schwinger–Dyson type diagram to represent mixings between different operators. All possible composite operators are assigned to each dotted part. $\hat{\lambda}$ is a matrix-valued vertex, and $\Sigma^{(g)}$ is a generalized 1PI (g -1PI) self-energy with respect to the composite operators.

It is a natural generalization of Equation (12) including an operator mixing. The diagonal component of \hat{G}_0 is the bare propagators of ϕ and ϕ^3 operators, respectively. $\hat{\lambda}$ is a matrix whose matrix element represents the coefficients of opening the ϕ^6 vertex. The coefficient for ϕ^3 to ϕ^3 in $\hat{\lambda}$ is given by $1/6 \times_6 C_3$. $\hat{\Sigma}^{(g)} = \hat{\Sigma}^{(g)}(\mathbf{k} = \mathbf{0}, k_{\parallel})$ is the \mathbb{Z}_2 -odd g-1PI function (In the \mathbb{Z}_2 -odd set of operators, and the $[\phi^5]$ operator does not appear in the mixing, though the ϕ^6 vertex can be decomposed into ϕ and ϕ^5 . It is because a diagram with $\langle \phi [\phi^5] \rangle$ is not 1PI while the g-1PI is 1PI as well in the ordinary sense). Namely, it consists of 1PI diagrams that do not contain bead diagrams shown in Figure 6. Such a generalization of the 1PI concept is mandatory since, in calculating the vertex contributions to EE, we need to open a vertex to take account of various channel contributions, and special care of the beads diagram in Figure 6 is necessary. This is the reason why we have generalized the concept of 1PI.

The above discussions can be straightforwardly extended to the contributions from \mathbb{Z}_2 -even operators, ϕ^2 and ϕ^4 . This case is simpler because the bare Green function is unity; $G^{(g)} = 1$. Then, we have the same matrix form

$$S_{\mathbb{Z}_2\text{-even}} = -\frac{V_{d-1}}{6} \int^{1/\epsilon} \frac{d^{d-1}k_{\parallel}}{2(2\pi)^{d-1}} \text{tr} \log \left(\hat{1} - \hat{\lambda} \hat{\Sigma}^{(g)} \right), \quad (16)$$

where, in this case, matrices are given by

$$\hat{\lambda} = \begin{pmatrix} 0 & -5\lambda_6/2 \\ -5\lambda_6/2 & 0 \end{pmatrix}, \quad \hat{\Sigma}^{(g)} = \begin{pmatrix} \Sigma_{\phi^2\phi^2}^{(g)} & \Sigma_{\phi^2\phi^4}^{(g)} \\ \Sigma_{\phi^4\phi^2}^{(g)} & \Sigma_{\phi^4\phi^4}^{(g)} \end{pmatrix}. \quad (17)$$

The coefficient comes from $5/2 = 1/6 \times_6 C_2$. It is a 2×2 matrix generalization of Equation (7). The g-1PI self-energy $\hat{\Sigma}^{(g)}$ does not contain bead diagrams, especially diagrams connected by the ϕ^6 vertex decomposed into ϕ^2 and ϕ^4 .

Note that EE of Equations (14) and (16) written in terms of the g-1PI functions can be rewritten in terms of the renormalized correlation functions as in the ϕ^4 case of Equations (4) and (9). The only difference is that we now have operator mixings and the relationship becomes more complicated. Let us explicitly check for the \mathbb{Z}_2 -odd case of Equation (14). It is rewritten as

$$\begin{aligned} S_{\mathbb{Z}_2\text{-odd}} &= \frac{V_{d-1}}{6} \int^{1/\epsilon} \frac{d^{d-1}k_{\parallel}}{2(2\pi)^{d-1}} \text{tr} \ln \left(\hat{G}_0 \frac{1}{\hat{1} - \hat{\lambda} \hat{\Sigma}^{(g)} \hat{G}_0} \right) \\ &= \frac{V_{d-1}}{6} \int^{1/\epsilon} \frac{d^{d-1}k_{\parallel}}{2(2\pi)^{d-1}} \text{tr} \ln \left(\hat{G}_0 + \hat{G}_0 \hat{\lambda} \hat{\Sigma}^{(g)} \hat{G}_0 + \hat{G}_0 \hat{\lambda} \hat{\Sigma}^{(g)} \hat{G}_0 \hat{\lambda} \hat{\Sigma}^{(g)} \hat{G}_0 + \dots \right). \end{aligned} \quad (18)$$

Writing the inside of the parenthesis as \tilde{G} , its matrix elements are given by

$$(\tilde{G})_{11} = G_0 + G_0 \Sigma^{(g)} G_0 + G_0 \Sigma_{\phi\phi^3}^{(g)} \left(-\frac{10}{3} \lambda_6 \right) \Sigma_{\phi^3\phi}^{(g)} G_0 + G_0 \Sigma^{(g)} G_0 \Sigma^{(g)} G_0 + \dots, \quad (19)$$

$$(\tilde{G})_{12} = G_0 \Sigma_{\phi\phi^3}^{(g)} + G_0 \Sigma^{(g)} G_0 \Sigma_{\phi\phi^3}^{(g)} + G_0 \Sigma_{\phi\phi^3}^{(g)} \left(-\frac{10}{3} \lambda_6 \right) \Sigma_{\phi^3\phi^3}^{(g)} + \dots, \quad (20)$$

$$(\tilde{G})_{21} = \left(-\frac{10}{3} \lambda_6 \right) \left(\Sigma_{\phi^3\phi}^{(g)} G_0 + \Sigma_{\phi^3\phi}^{(g)} G_0 \Sigma^{(g)} G_0 + \Sigma_{\phi^3\phi^3}^{(g)} \left(-\frac{10}{3} \lambda_6 \right) \Sigma_{\phi^3\phi}^{(g)} G_0 + \dots \right), \quad (21)$$

$$(\tilde{G})_{22} = 1 + \left(-\frac{10}{3} \lambda_6 \right) \left(\Sigma_{\phi^3\phi^3}^{(g)} + \Sigma_{\phi^3\phi}^{(g)} G_0 \Sigma_{\phi\phi^3}^{(g)} + \Sigma_{\phi^3\phi^3}^{(g)} \left(-\frac{10}{3} \lambda_6 \right) \Sigma_{\phi^3\phi^3}^{(g)} + \dots \right). \quad (22)$$

We can explicitly see that the sum of g-1PI's in each matrix element is combined into the ordinary 1PI functions Σ 's, and hence can be written by the renormalized correlation functions as

$$(\tilde{G})_{11} = G_0 + G_0 \Sigma G_0 + G_0 \Sigma G_0 \Sigma G_0 + \dots = G, \quad (23)$$

$$(\tilde{G})_{12} = (G_0 + G_0 \Sigma G_0 + G_0 \Sigma G_0 \Sigma G_0 + \dots) \Sigma_{\phi\phi^3} = G_{\phi\phi^3}, \quad (24)$$

$$(\tilde{G})_{21} = \left(-\frac{10}{3} \lambda_6 \right) \Sigma_{\phi^3\phi} (G_0 + G_0 \Sigma G_0 + G_0 \Sigma G_0 \Sigma G_0 + \dots) = -\frac{10}{3} \lambda_6 G_{\phi^3\phi}, \quad (25)$$

$$(\tilde{G})_{22} = 1 + \left(-\frac{10}{3} \lambda_6 \right) (\Sigma_{\phi^3\phi^3} + \Sigma_{\phi^3\phi} G \Sigma_{\phi\phi^3}) = 1 - \frac{10}{3} \lambda_6 G_{\phi^3\phi^3}. \quad (26)$$

As a result, Equation (14) can be summarized as

$$S_{\mathbb{Z}_2\text{-odd}} = \frac{V_{d-1}}{6} \int^{1/\epsilon} \frac{d^{d-1}k_{\parallel}}{2(2\pi)^{d-1}} \text{tr} \log [\hat{I} + \hat{\lambda} \hat{G}], \quad (27)$$

where

$$\hat{I} = \begin{pmatrix} 0 & 0 \\ 0 & 1 \end{pmatrix}, \quad \hat{\lambda} = \begin{pmatrix} 1 & 0 \\ 0 & -10\lambda_6/3 \end{pmatrix}, \quad \hat{G} = \begin{pmatrix} G & G_{\phi\phi^3} \\ G_{\phi^3\phi} & G_{\phi^3\phi^3} \end{pmatrix}. \quad (28)$$

The same discussion can be applied to Equation (16). This gives an alternative, unified formula for EE in terms of the renormalized Green functions.

3.2. $\phi^4 + \phi^6$ Theory and Further Generalizations

Let us generalize a bit more and consider a case when the Lagrangian contains two interaction terms

$$\mathcal{L}_{pot} = \frac{\lambda_4}{4} \phi^4 + \frac{\lambda_6}{6} \phi^6. \quad (29)$$

As in the ϕ^6 theory, we need to consider three composite operators, ϕ^2 , ϕ^4 , and ϕ^3 , in order to take into account contributions to EE from these vertices. Again, we have \mathbb{Z}_2 invariance, and EE is a sum of \mathbb{Z}_2 -even and odd contributions. The \mathbb{Z}_2 -odd contribution is given by

$$S_{\mathbb{Z}_2\text{-odd}} = -\frac{V_{d-1}}{6} \int^{1/\epsilon} \frac{d^{d-1}k_{\parallel}}{2(2\pi)^{d-1}} \text{tr} \log \left[\hat{G}_0^{-1} - \begin{pmatrix} 1 & 0 \\ 0 & -10\lambda_6/3 \end{pmatrix} \begin{pmatrix} \Sigma^{(g)} & \Sigma_{\phi\phi^3}^{(g)} \\ \Sigma_{\phi^3\phi}^{(g)} & \Sigma_{\phi^3\phi^3}^{(g)} \end{pmatrix} \right], \quad (30)$$

where \hat{G}_0 is the same as in Equation (15) while \mathbb{Z}_2 -even contribution is given by

$$S_{\mathbb{Z}_2\text{-even}} = -\frac{V_{d-1}}{6} \int^{1/\epsilon} \frac{d^{d-1}k_{\parallel}}{2(2\pi)^{d-1}} \text{tr} \log \left[\hat{I} - \begin{pmatrix} -3\lambda_4/2 & -5\lambda_6/2 \\ -5\lambda_6/2 & 0 \end{pmatrix} \begin{pmatrix} \Sigma_{\phi^2\phi^2}^{(g)} & \Sigma_{\phi^2\phi^4}^{(g)} \\ \Sigma_{\phi^4\phi^2}^{(g)} & \Sigma_{\phi^4\phi^4}^{(g)} \end{pmatrix} \right]. \quad (31)$$

Now, a generalization to e.g., ϕ^{2n} vertices with higher n is evident. The propagator and vertex contributions to EE are unified to be written in a matrix form as Equation (14):

$$S_{EE} = -\frac{V_{d-1}}{6} \int^{1/\epsilon} \frac{d^{d-1}k_{\parallel}}{2(2\pi)^{d-1}} \text{tr} \log [(\hat{G}_0^{-1} - \hat{\lambda} \hat{\Sigma}^{(g)}) (\mathbf{k} = 0, k_{\parallel})]. \quad (32)$$

The size of matrices becomes larger as a larger number of operators are mixed, and each set of mixed operators forms a block diagonal component. \hat{G}_0 is a diagonal matrix whose entry is mostly 1 except the fundamental field. $\hat{\lambda}$ represents a mixing among operators via vertices while $\hat{\Sigma}^{(g)}$ represents amputated correlators of all the fundamental and composite operators. The notion of the g-1PI is also extended to exclude all the bead diagrams constructed by all the vertices along with the ordinary non-1PI diagrams. This form of EE contains all the contributions from the propagators and the vertices. We provide the derivation in Appendix B.

An essential point is that we can rewrite Equation (32) in terms of the renormalized correlation functions in the same manner as in Equation (27) as

$$S_{EE} = \frac{V_{d-1}}{6} \int^{1/\epsilon} \frac{d^{d-1}k_{\parallel}}{2(2\pi)^{d-1}} \text{tr} \ln(\tilde{I} + \hat{\lambda}\hat{G}). \quad (33)$$

Here, $\tilde{I} = \text{diag}(0, 1, \dots, 1)$, \hat{G} is the matrix form of the correlators of operators, and we have arranged the elements of the matrices so that the first line and first column involve the fundamental field ϕ . The size of the matrices is finite as far as there is a finite number of vertices. In the ϕ^n -theory, we need to consider only the composite operators $[\phi^j]$ with $j \leq n - 2$, which appear to open vertices.

3.3. Derivative Interactions

Special care is necessary for generalizations with derivative interactions since composite operators with Lorentz indices appear. Let us consider the following interaction as an example:

$$\mathcal{L}_{pot} = \frac{\lambda_{\partial}}{4} (\phi \partial \phi)^2. \quad (34)$$

In this case, the two types of scalar composite operators, $[\phi^2]$ and $[(\partial\phi)^2]$, as well as a spin-1 operator $[\phi \partial_{\mu} \phi]$ appear from an opened vertex. Since the spin-1 operator does not mix with either ϕ or $[\phi^2]$ or $[(\partial\phi)^2]$, we can separately study its contribution to EE. Thus, we have three block-diagonal sectors.

The spin-0 sectors can be treated as before. Thus, let us focus on the spin-1 sector. The formula Equation (32) gets a bit modified since EE of a spinning field is different from that of a scalar field due to the rotation of the internal spin induced by \mathbb{Z}_M twist, and hence an extra phase appears in evaluating EE [47]. The operator $J_{\mu} := [\phi \partial_{\mu} \phi]$ is decomposed into its two-dimensional part J and $(d-1)$ -dimensional part J_i . The latter is a scalar on the two-dimensional spacetime normal to the boundary and can be treated as in Equation (32). On the other hand, the contribution to EE from the two-dimensional vector J is modified. From Equation (2.21) in [47], the coefficient of EE is proportional to

$$c_{\text{eff}}^{\text{boson}}(s) = \frac{1}{4} \frac{\partial J(s, M)}{\partial M} \Big|_{M=1} = \frac{1}{6} - \frac{|s|}{2} \quad (35)$$

for a bosonic field with spin s . This coefficient c_{eff} replaces the coefficient of $1/6$ in front of Equation (5). Thus, for $(d+1)$ -dimensional vector J_{μ} , the total coefficient is given by $(d-1)/6 + 2(1/6 - 1/2) = (d-5)/6$. Therefore, the propagator and vertex contributions to EE with this derivative interaction are given by either of the following two forms:

$$\begin{aligned} S_{EE} &= -\frac{V_{d-1}}{6} \int^{1/\epsilon} \frac{d^{d-1}k_{\parallel}}{2(2\pi)^{d-1}} \text{tr} \left(S \log \left[\hat{G}_0^{-1} - \hat{\lambda} \hat{\Sigma}^{(g)} \right] \right) \\ &= \frac{V_{d-1}}{6} \int^{1/\epsilon} \frac{d^{d-1}k_{\parallel}}{2(2\pi)^{d-1}} \text{tr} (S \log [\tilde{I} + \hat{\lambda} \hat{G}]), \end{aligned} \quad (36)$$

where

$$S = \begin{pmatrix} 1 & 0 & 0 & 0 \\ 0 & 1 & 0 & 0 \\ 0 & 0 & 1 & 0 \\ 0 & 0 & 0 & (d-5) \end{pmatrix}, \quad \tilde{I} = \begin{pmatrix} 0 & 0 & 0 & 0 \\ 0 & 1 & 0 & 0 \\ 0 & 0 & 1 & 0 \\ 0 & 0 & 0 & 1 \end{pmatrix}, \quad \hat{\lambda} = \begin{pmatrix} 1 & 0 & 0 & 0 \\ 0 & 0 & -\lambda_{\partial} & 0 \\ 0 & -\lambda_{\partial} & 0 & 0 \\ 0 & 0 & 0 & -\lambda_{\partial}/2 \end{pmatrix},$$

$$\hat{G} = \begin{pmatrix} G & 0 & 0 & 0 \\ 0 & G_{\phi^2\phi^2} & G_{\phi^2(\partial\phi)^2} & 0 \\ 0 & G_{(\partial\phi)^2\phi^2} & G_{(\partial\phi)^2(\partial\phi)^2} & 0 \\ 0 & 0 & 0 & G_{(\phi\partial_\mu\phi)(\phi\partial^\mu\phi)} \end{pmatrix}. \quad (37)$$

S is an additional coefficient due to the spin. Here, we have summed over $(d+1)$ -dimensional vector contributions, but, generally speaking, it is more convenient to write a matrix corresponding to each irreducible representation of the two-dimensional rotation with spin s . According to [47], the coefficient c for fermions with odd half-integer spin s is given by $c_{\text{eff}}^{\text{fermion}}(s) = -1/3$. Thus, if we treat each two-dimensional spin component as an independent field, the diagonal component of the matrix $S/6$ is given by $c_{\text{eff}}^{\text{boson/fermion}}(s)$ for each spin s field.

4. IR Behavior of EE and Wilsonian Effective Action

Thus far, we have succeeded to extract contributions to EE, particularly from propagators of fundamental fields and vertices, and its most general form is given by the unified matrix form in Equation (36). Thus, if we can calculate correlators $\hat{\Sigma}^{(g)}$ or \hat{G} , we can obtain their contributions to EE. These contributions to EE are, however, a part of the whole EE in the framework of the \mathbb{Z}_M gauge theory on Feynman diagrams, and we wonder how we can extract the other contributions to EE. In this section, we give a conjecture that the IR part of EE is exhausted by summing all the vertex contributions (together with propagator contributions) constructed from the IR Wilsonian effective action.

4.1. More Properties of Vertex Contributions to EE

First, note that the leading order term of the vertex contribution corresponding to composite operators $\{\mathcal{O}_n\}$ is perturbatively given by expanding the logarithm as

$$\begin{aligned} S_{\text{vertex}} &= \frac{V_{d-1}}{12} \int \frac{d^{d-1}k_\parallel}{(2\pi)^{d-1}} \text{tr } \hat{\lambda} \hat{\Sigma}^{(g)}(\mathbf{k} = 0, k_\parallel) \\ &= \frac{V_{d-1}}{12} \int d^2\mathbf{r} \sum_{m,n} (\hat{\lambda})_{mn} \langle \mathcal{O}_n(-\frac{\mathbf{r}}{2}, x_\parallel = 0) \mathcal{O}_m(\frac{\mathbf{r}}{2}, x_\parallel = 0) \rangle^{(g)}. \end{aligned} \quad (38)$$

The integral in the second line reflects the property of a twisted propagator that its center coordinate is pinned at the boundary $x_\parallel = 0$ with two loose ends. For more detailed discussions, see [42,43]. For instance, when $\mathcal{O} = [\phi^2]$, the leading perturbative term is given by using the renormalized propagator G of the fundamental field ϕ as

$$S_{\text{vertex}} \sim \frac{V_{d-1}}{6} \int d^2\mathbf{r} \left(-\frac{3\lambda_4}{2} \right) G(\mathbf{r}, 0)^2. \quad (39)$$

$-3\lambda_4/2$ is the component of $\hat{\lambda}$ which associates $[\phi^2]$ to $[\phi^2]$. If we consider an operator such as $\mathcal{O} = [\phi^n]$, the integrand is proportional to $G(\mathbf{r}, 0)^n$ and decays faster for a larger n . This means that, at least perturbatively, higher-dimensional composite operators tend to contribute less to EE.

Another important point to note in Equation (33), particularly for its vertex part, is that, if some composite operators in $\hat{\lambda}\hat{G}$ dominate 1 in the logarithm in a strong coupling region, the contribution from the composite operator can be approximated as

$$\text{tr } \log(\hat{1} + \hat{\lambda}\hat{G}) \sim \text{tr } \log(\hat{G}) \quad (40)$$

up to a constant depending on the coupling constant. Then, EE can be written as a logarithm of renormalized correlators similar to the fundamental field. There is no explicit dependence on the coupling constant other than the overall factor and its dependence is only given through the renormalization of correlators.

4.2. Wilsonian RG and EE: Free Field Theories

Now, we discuss the issue of other contributions to EE besides the propagators and vertices. For this purpose, it is convenient to utilize the concept of the Wilsonian renormalization group (RG) to the effective field theory in the IR region [40,41] (A modern approach for the Wilsonian RG is given by the functional RG method [48,49]). In the Wilsonian RG, we first divide the momentum domain into low and high regimes. Schematically,

$$k \in [0, \Lambda] = [0, e^{-t}\Lambda] + [e^{-t}\Lambda, \Lambda] \quad (41)$$

with $t > 0$ and then it integrates quantum fluctuations over the high regimes. Then, we rescale the momentum $k \rightarrow k' = e^t k$ so that $k' \in [0, \Lambda]$. In this procedure, the original parameters in the action are renormalized, e.g.,

$$m \rightarrow m', \quad \lambda_4 \rightarrow \lambda'_4. \quad (42)$$

In addition, new interaction terms appear, e.g., in the ϕ^4 theory in $(3+1)$ dimensions,

$$\lambda_6 \frac{\phi^6}{\Lambda^2}, \quad \lambda_\partial \frac{(\phi \partial \phi)^2}{\Lambda^2}, \quad \lambda_8 \frac{\phi^8}{\Lambda^4} \dots \quad (43)$$

First, let us look at what happens for a free theory. For a free scalar field with a mass m , EE is simply given by

$$S_{\text{EE}}(\Lambda) = -\frac{V_{d-1}}{12} \int^\Lambda \frac{d^{d-1}k_{\parallel}}{(2\pi)^{d-1}} \log \left[(k_{\parallel}^2 + m^2)/\Lambda^2 \right]. \quad (44)$$

By integrating the high momentum region, nothing happens except fluctuations of that region are discarded:

$$S_{\text{EE}}(e^{-t}\Lambda) = -\frac{V_{d-1}}{12} \int^{e^{-t}\Lambda} \frac{d^{d-1}k_{\parallel}}{(2\pi)^{d-1}} \log \left[e^{2t}(k_{\parallel}^2 + m^2)/\Lambda^2 \right]. \quad (45)$$

Then, we rescale the momentum as $k' = e^t k$ to obtain

$$S'_{\text{EE}}(\Lambda) = -\frac{V_{d-1}}{12} \int^\Lambda \frac{d^{d-1}k'_{\parallel}}{e^{(d-1)t} \times (2\pi)^{d-1}} \log \left[(k'^2_{\parallel} + e^{2t}m^2)/\Lambda^2 \right]. \quad (46)$$

Of course, for a free field theory, it is equal to Equation (44) with the integration range $[0, e^{-t}\Lambda]$. For an interacting theory, it is different since high and low momentum modes are entangled. We continue the integration over high momentum modes until $e^{-t}\Lambda = m$. Then, EE is given by Equation (44) with the integration range $[0, m]$. It gives the IR part of the EE at the scale m , and the discarded parts in higher momentum are UV cut-off dependent. By performing the momentum integration, the EE at the scale m is now given by

$$S_{\text{EE}}^{\text{IR}}(m) \equiv -\frac{V_{d-1}}{12} \int^m \frac{d^{d-1}k_{\parallel}}{(2\pi)^{d-1}} \log \left[(k_{\parallel}^2 + m^2)/\Lambda^2 \right] \quad (47)$$

$$= \frac{N_{\text{eff}} V_{d-1}}{12} m^{d-1} \log \left[\tilde{\Lambda}^2/m^2 \right], \quad (48)$$

where $\tilde{\Lambda}$ is proportional to the UV cutoff as $\tilde{\Lambda} = \Lambda \exp \left[\Phi(-1, 1, \frac{d+1}{2})/2 \right] / \sqrt{2}$. $\Phi(z, s, \alpha) \equiv \sum_{n=0}^{\infty} z^n / (n + \alpha)^s$ is the Lerch transcendent. For example, in $d = 3$, it is given by

$\tilde{\Lambda} = e^{1/2}\Lambda/2$. Equation (48) coincides with the ordinary universal term in even space-time dimensions. V_{d-1} is the area of the boundary and

$$N_{\text{eff}} = \left(\frac{1}{2}\right)^{d-1} \frac{1}{\pi^{(d-1)/2} \Gamma((d+1)/2)} \quad (49)$$

is the effective number of degrees of freedom that can contribute to EE in the IR. The result of Equation (48) indicates that the universal part of EE originates in the quantum correlations of fields whose length scale is larger than the typical correlation length $\xi = 1/m$ of the system. $S_{\text{EE}}^{\text{IR}}(m)$ becomes larger for smaller masses m .

4.3. Wilsonian RG and EE: Interacting Field Theories

In the free case, the Wilsonian RG can extract the IR behavior of EE that is independent of the UV cutoff. In the Wilsonian RG, quantization is gradually performed from high momentum to low, and in the IR limit, all fluctuations are integrated out so that all the loop effects are incorporated in the Wilsonian effective action (EA). The Wilsonian EA becomes more and more complicated as radiative corrections are gradually taken into account. Thus, we can expect that all the contributions to EE are encoded in the Wilsonian EA. We conjecture that EE is given by a sum of all the propagator and vertex contributions in the Wilsonian EA.

In the following, we focus on the IR limit of the Wilsonian EA. Let us recall a simple case in Equation (10). The correlator $G_{\phi^2\phi^2}$ is graphically given by the upper figure of Figure 9, and the first term is given by Equation (39). This diagram is present even in the IR limit where all the fluctuations are integrated out since it is simply connected by the propagators of the fundamental field. The other terms vanish in the IR limit of the Wilsonian RG since they are quantum corrections to the first classical term. After all the fluctuations are integrated out, further quantum corrections should be absent because such effects are already absorbed in the Wilsonian EA. Thus, we expect that the vertex contributions of the composite operator, e.g., ϕ^2 , are drastically simplified in the IR limit in which we can replace the Green function $G_{\phi^2\phi^2}$ by the leading diagrams as shown in the lower figure of Figure 9. After all, the vertex contribution in Equation (10) becomes

$$S_{\text{vertex}} = -\frac{V_{d-1}}{12} \int^{\Lambda} \frac{d^{d-1}k_{\parallel}}{(2\pi)^{d-1}} \log \left[1 + 3\lambda_4 \int \frac{d^{d+1}p}{(2\pi)^{d+1}} G(p)G(-p, k_{\parallel} - p_{\parallel}) \right] \quad (50)$$

in the IR limit. The coupling constant λ_4 is the renormalized one since it is a coefficient of Wilsonian EA in the IR limit. (We have already taken quantum fluctuations into account and eliminated the UV divergences in coupling constants and observables in the IR limit, but another UV divergences appear in the calculation of EE since we need to sum all the momentum modes. It is also necessary even for the free theory, and indeed we extracted the IR universal part by subtracting cutoff dependent terms). As in the free case, we separate the vertex contributions into IR and UV parts. The IR part is defined similarly by restricting the integration range from $k_{\parallel} \in [0, \Lambda]$ to $[0, m]$. Instead, we may integrate up to $1/\xi_{\phi^2}$, where ξ_{ϕ^2} is the correlation length of the operator $[\phi^2]$. The difference is a matter of definition of the IR universal part of EE, and we need a precise prescription to subtract the cutoff dependent terms in EE. For example, we may take a variation with respect to the mass m and then integrate to obtain the universal part of EE. In this definition, we need to know how ξ_{ϕ^2} and m are related. This is under investigation in moment.

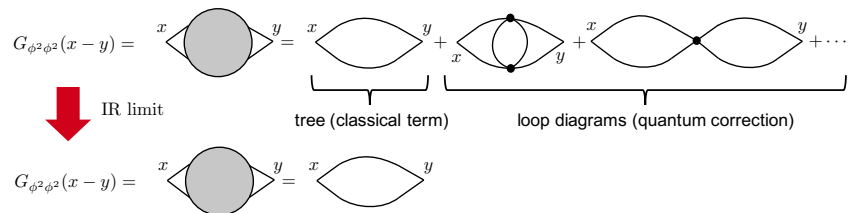


Figure 9. The upper figure shows Feynman diagrams constituting $G_{\phi^2 \phi^2}$. Only the leading diagram survives in the IR limit.

In general, of course, we need to take operator mixings into account, but the generalization is straightforward. We will investigate more detailed behaviors of EE in the infrared limit of the Wilsonian EA for a concrete model. The final question is whether there are contributions to EE other than the vertex contributions in the Wilsonian EA. In the formulation of EE based on the \mathbb{Z}_M gauge theory on Feynman diagrams, vertex contributions are only a part of all the contributions to EE. However, in the IR limit of Wilsonian RG, all the quantum fluctuations are integrated out, and we do not need to evaluate loop diagrams: all the Feynman diagrams are tree diagrams. Thus, the vertex contributions, as well as the propagator contributions, to EE must suffice for the IR behavior of EE. We will investigate further issues of the RG flow of EE in a separate paper [50].

5. Conclusions

This is the third paper in a series of our investigations on EE in interacting field theories based on the notion of the \mathbb{Z}_M gauge theory on Feynman diagrams, proposed in [42] and extended in [43]. In the previous papers, we have focused on two important contributions to EE: one from the propagators of the fundamental field and another from vertices which can be interpreted as correlations of composite operators. In this paper, we have further extended the results to include effects of mixings of various composite operators as well as the original fundamental fields. The final formula of EE is given in a unified matrix form. We then discuss an implication to the IR behavior of EE from the Wilsonian RG approach to effective field theories. We conjecture that the IR part of EE in interacting field theories is given by a sum of all vertex contributions in the Wilsonian effective action. In this context, it is interesting to look at the relation to the variational method of EE [28–30,51]. In this approach, EE of interacting field theories is expressed in terms of a non-Gaussian deformation of the Gaussian vacuum wave function. This deformation must be related to the vertex contributions we have found.

Author Contributions: All authors (S.I., T.M. and K.S.) have equally contributed to this manuscript. All authors have read and agreed to the published version of the manuscript.

Funding: This work is in part supported by the Grant-in-Aid for Scientific research, No. 18H03708 (S.I.), No. 16H06490 (S.I.), No. 20J00079 (K.S.).

Institutional Review Board Statement: Not applicable.

Informed Consent Statement: Not applicable.

Data Availability Statement: Not applicable.

Acknowledgments: We thank Masahiro Hotta, Jun Nishimura, Takuma Nishioka, Yoshiki Sato, Kengo Shimada, Sotaro Sugishita, Takao Suyama, Tadashi Takayanagi, and Kazuya Yonekura for their discussions. We also acknowledge the referee of PRD to the previous papers whose comments have stimulated the present investigations. We are supported in part by the Grant-in-Aid for Scientific research, No. 18H03708 (S.I.), No. 16H06490 (S.I.), No. 20J00079 (K.S.) and SOKENDAI.

Conflicts of Interest: The authors declare no conflict of interest.

Appendix A. Area Laws for Rényi Entropy and Entanglement Capacity

In this appendix, we show that the area law (In general, the area law means $O(|\partial A|)$; the quantity scales at most as the area [52]). $S_{EE} \propto \text{vol}(\partial A)$ ($\sim V_{d-1}$ in our setup) holds at the level of Rényi entropy $S_n \equiv \frac{1}{1-n} \log \text{Tr} \rho_A^n$. We can apply the same discussion performed in our previous papers [42,43] deriving the area law for EE. First, to apply the orbifold method introduced in Section 2.1, we rewrite $S_{n=1/M}$ in terms of free energy $F^{(M)}$ on $\mathbb{R}^2/\mathbb{Z}_M \times \mathbb{R}^{d-1}$:

$$S_{1/M} = \frac{1}{M-1} (F^{(1)} - M F^{(M)}). \quad (\text{A1})$$

Based on the \mathbb{Z}_M gauge theory on Feynman diagrams introduced in Section 2.1, the number of independent twists is given by the number of loops L in the Feynman diagrams even though every propagator is originally twisted. Let us denote the number of initial twists or equivalently the number of propagators by P . Twists other than the independent ones can be eliminated by the redundancy at vertices. The number of such redundant twists is given by $P - L = V - 1$, where the number of vertices is denoted by V . As a result, the $1/M$ factor from each vertex is almost canceled except one by the trivial summation for $(V - 1)$ redundant twists. Furthermore, the overall momentum conservation yields the sum of L twisted momenta equal to the original one. In short, any Feynman diagrams contributing to $F^{(M)}$ are expressed as

$$\frac{V_{d-1}}{M} \sum_{\{m\}} \int \prod_{l=1}^L \left[\frac{d^2 p_l}{(2\pi)^2} \right] I(\{\mathbf{p}\}; \{m\}) \delta^2 \left(\sum_{l=1}^L (1 - \hat{g}^{m_l}) \mathbf{p}_l \right), \quad (\text{A2})$$

where $\sum_{\{m\}}$ is a summation over all twists—each from 0 to $M - 1$. $I(\{\mathbf{p}\}; \{m\})$ is some function of momenta and twists.

When all m 's are zero, no momenta are twisted. Such diagrams constitute nothing but $F^{(1)}/M$. Although this contribution in $F^{(M)}$ is proportional to V_{d+1} and seemingly violates the area law, it is canceled in $S_{1/M}$ in Equation (A1). Other configurations of twists include at least one nonzero twist. As a result, the argument of the delta function in Equation (A2) is always nonzero, and it combined with I carries a nontrivial dependence in M after the summation over twists. Unless an explicit calculation is done, we do not know the precise M dependence of Equation (A2) or $S_{1/M}$. Nevertheless, since terms contributing to $S_{1/M}$ always have nonzero arguments of the delta function, there is no more volume factor other than V_{d-1} . If M can be analytically continued to $M = 1/n$, this completes the proof of the area law for Rényi entropy S_n .

The proof above only depends on the technique of Feynman diagrams and thus the area law for Rényi entropy is proven for any locally interacting QFTs, given a half space as a subregion.

It is worthwhile to note that the area law for Rényi entropy immediately implies the area law for the capacity of entanglement [44,45],

$$\begin{aligned} C_A &\equiv \lim_{n \rightarrow 1} n^2 \frac{\partial^2}{\partial n^2} \log \text{Tr} \rho_A^n \\ &= \frac{\partial^2}{\partial n^2} [(1 - n) S_n] \Big|_{n \rightarrow 1} \\ &= 2 \frac{\partial S_{1/M}}{\partial M} \Big|_{M \rightarrow 1} \end{aligned} \quad (\text{A3})$$

as well as EE since C_A is linear in Rényi entropy. Since C_A is alternatively written as the fluctuation of the modular Hamiltonian $-\log \rho_A$, it is more sensitive to the change of dominant contributions in the replicated geometry and recently discussed in the context of the black hole evaporation [53–55]. It is interesting if we can compute such quantities in interacting theories and follow the behavior of higher orders in M .

Although the area law itself is intuitive for physicists as entanglement across the boundary ∂A should be dominant for any local QFTs, the proof of this is difficult; a general proof is known only for gapped systems in $(1 + 1)$ dimensions [56]. It is remarkable that we can show the area law of both EE and Rényi entropy in any locally interacting theories.

As a further generalization, it is intriguing to relax several assumptions and see how the EE and Rényi entropy deviate from the area law. In our setup, ∂A is smooth, the interactions are local, and the system is translationally invariant. Some cases are known where the above features are not satisfied, and the area law is violated. For example, when the entangling surface ∂A has a singular geometry, a logarithmic correction appears (see [57] for example). For (non-)Fermi liquid theories [58], another logarithmic violation to the area law is known. For nonlocal [59] or non-translationally invariant [60,61] systems, the volume law instead of the area law of EE has been confirmed. To see the transition from the area law to the volume law, Lifshitz theories [62–64] might be an interesting playground as it possesses a nonlocal feature in some limit.

Appendix B. Proof of the EE Formulae of the Vertex Contributions

In the body of the paper, we have used the general formula for the vertex contributions to EE, such as in Equation (32). In this appendix, we prove that this formula gives all the contributions of a single vertex twist. In the case of the propagator contributions, the general formula is given by Equation (5), and the proof that all the single twist contributions are summarized by the 1-loop expression is given in the 2PI framework in the previous papers [42,43]. For the vertex contributions, when auxiliary fields can be introduced, the proof is same, however, in general cases when various channels in the opened vertices are mixed, we need a different proof. In this appendix, we give a diagrammatic proof.

First, let us remind of the redundancies of assigning the flux m of the plaquette to a twist of the propagators in the 1-loop diagram in Figure 2i. In this case, due to the \mathbb{Z}_M gauge invariance at each vertex connecting propagators, the flux can twist only one of the propagators—not more than one—and this gives the coefficient $1/n$ in the expansion of Equation (5). The same happens for the vertex contributions. The configurations illustrated in Figure 4 are interpreted as the vertex contributions to EE, but a similar redundancy will occur when the corresponding composite operators form a 1-loop type diagram. Thus, in order for the proof, we will take the following two steps: (i) summing all the vertex contributions as if all of them are independent and then (ii) taking account of the redundancies to obtain the correct vertex contributions. This two-step proof shows that only the 1-loop type contributions in Equation (32) survive. The proof is similar to the one based on the 2PI formalism.

Let us begin with the fundamental relation between the free energy and an n -point vertex. Suppose that we have an n -point interaction vertex whose action is given by

$$(\text{action}) = \frac{1}{2} \int d^{d+1}x \phi G_0^{-1} \phi + \dots + \frac{\lambda_n}{n} \int \prod_{i=1}^n d^{d+1}x_i V_{n0}(x_1, \dots, x_n) \phi(x_1) \dots \phi(x_n), \quad (\text{A4})$$

$$V_{n0}(x_1, \dots, x_n) = \int d^{d+1}y \prod_{i=1}^n \delta^{d+1}(y - x_i). \quad (\text{A5})$$

Then, we have the equation

$$\frac{\delta F}{\delta V_{n0}(x_1, \dots, x_n)} = \frac{\lambda_n}{n} \langle \phi(x_1) \dots \phi(x_n) \rangle, \quad (\text{A6})$$

where F is the free energy and the right-hand side is the exact n -point function multiplied by the coupling constant.

In order to evaluate the EE contributions from twisting vertices, let us first sum all the contributions as if they were independent. This can be done by taking a variation of bubble diagrams (free energy) with respect to the tree-level interaction vertex, and

then reconnecting the endpoints by a set of free propagators as in the leftmost figure in Figure A1.

According to Equation (A6), if we naively summed all the contributions to EE from opening all the λ_n -vertices, EE would be given by

$$\begin{aligned} S_{\lambda_n}^{(\text{naive})} &= - \int d^{d+1}x d^{d+1}y \partial_M \left(\sum_{m=1}^{M-1} \delta^{d+1}(\hat{g}^m x - y) \right) \Big|_{M \rightarrow 1} \\ &\quad \times \frac{\lambda_n}{n} \frac{1}{2} \left\{ C_{2,n-2}^{(n)} \langle [\phi^2](x) [\phi^{n-2}](y) \rangle + C_{3,n-3}^{(n)} \langle [\phi^3](x) [\phi^{n-3}](y) \rangle + \dots \right\} \\ &= - \frac{V_{d-1}}{12} \int \frac{d^{d-1}k_{\parallel}}{(2\pi)^{d-1}} \frac{\lambda_n}{n} \left\{ C_{2,n-2}^{(n)} G_{\phi^2 \phi^{n-2}}(\mathbf{0}; k_{\parallel}) + C_{3,n-3}^{(n)} G_{\phi^3 \phi^{n-3}}(\mathbf{0}; k_{\parallel}) + \dots \right\}, \end{aligned} \quad (\text{A7})$$

where $C_{2,n-2}^{(n)}$, $C_{3,n-3}^{(n)}$, ... are combinatorial factors to reconnect the endpoints. Endpoints can be decomposed into two sets as in Figure A1 and then regarded as a composite operator. In the definition of $C_{2,n-2}^{(n)}$, etc., we distinguish the left and right sets of endpoints, x and y , for later convenience, and thus divide by 2 in the second line of Equation (A7) to avoid an overcounting.

Here, note that we should not include a decomposition of n endpoints ϕ^n into (ϕ, ϕ^{n-1}) because it does not correspond to opening a vertex, rather it generates a non-1PI diagram in the ordinary sense. Such contributions would lead to an overcounting of the propagator contributions. In addition, note that we should not consider a reconnection of n endpoints in which some of them do not participate in the propagation of the composite operator; e.g., a diagram such that a pair of endpoints forms a closed loop and the other $n-2$ endpoints are decomposed into two sets to form the propagator of the composite operator. These kinds of diagrams are absorbed into the renormalizations of the coupling constant λ_{n-2} .

Now, let us go to step 2 to obtain the correct vertex contributions. $S_{\lambda_n}^{(\text{naive})}$ is not the correct one because of the redundancies we neglected. Let us consider the effects of redundancies separately for each type of composite operator in Equation (A7).

For simplicity, let us consider the $G_{\phi^k \phi^k}$ -type contribution in Equation (A7) which emerges from a $2k$ -point vertex by decomposing into 2 sets of k and k . We simply assume that it is not mixed with other operators here. The simplest example is $[\phi^2]$ in the ϕ^4 -theory, as described in Section 2.3. If the redundancies were neglected, the contribution to EE from this operator naively would take the form

$$S_{\lambda_{2k}}^{(\text{naive})} \Big|_{\phi^k \phi^k} = - \frac{V_{d-1}}{12} \int \frac{d^{d-1}k_{\parallel}}{(2\pi)^{d-1}} \frac{\lambda_{2k}}{2k} C_{k,k}^{(2k)} G_{\phi^k \phi^k}(\mathbf{0}; k_{\parallel}). \quad (\text{A8})$$

Reflecting the twisting of the composite operator, the Green function is restricted to $k = \mathbf{0}$ modes. The Green function can be expanded with respect to the g-1PI self-energy introduced in Section 2.3 as (For a consistent expansion, we have defined the combinatorics factors (C 's) by distinguishing the two endpoints:)

$$\begin{aligned} G_{\phi^k \phi^k} &= \Sigma_{\phi^k \phi^k}^{(g)} + \Sigma_{\phi^k \phi^k}^{(g)} \left(-\frac{\lambda_{2k}}{2k} C_{k,k}^{(2k)} \right) \Sigma_{\phi^k \phi^k}^{(g)} \\ &\quad + \Sigma_{\phi^k \phi^k}^{(g)} \left(-\frac{\lambda_{2k}}{2k} C_{k,k}^{(2k)} \right) \Sigma_{\phi^k \phi^k}^{(g)} \left(-\frac{\lambda_{2k}}{2k} C_{k,k}^{(2k)} \right) \Sigma_{\phi^k \phi^k}^{(g)} + \dots \end{aligned} \quad (\text{A9})$$

The correct formula must take the redundancies caused by \mathbb{Z}_M gauge invariance into account. Such redundancies occur in the above expansion of Equation (A9) when there are more than one $\Sigma_{\phi^k \phi^k}^{(g)}$ as shown in Figure A1. The coefficients of these terms in Equation (A9) over count the effects of the twist.

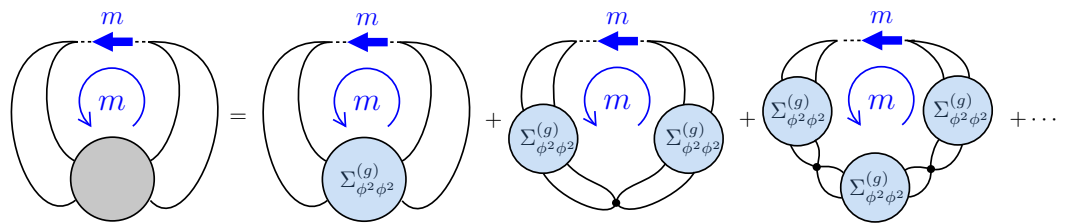


Figure A1. Graphical expression of Equations (A8) and (A9) for $k = 2$ in the ϕ^4 -theory. The gray blob on the left-hand side is the exact four-point correlation function. The dotted line denotes a twisted delta function to open the vertex. The twist of the diagram is given by the flux m in the center circle. On the right-hand side, the twist is made associated with the propagator of a composite operator in the opened vertex. If we would open all the vertices on the circled line and take all the contributions to EE, it would give an overcounting of EE.

The resolution to avoid the overcounting is simple. For the term consisting of m g-1PI parts in Equation (A7), we should divide it by m . Consequently, by replacing $G_{\phi^k \phi^k}$ in the naive estimation Equation (A8) with

$$\begin{aligned} \Sigma_{\phi^k \phi^k}^{(g)} + \frac{1}{2} \Sigma_{\phi^k \phi^k}^{(g)} \left(-\frac{\lambda_{2k}}{2k} C_{k,k}^{(2k)} \right) \Sigma_{\phi^k \phi^k}^{(g)} \\ + \frac{1}{3} \Sigma_{\phi^k \phi^k}^{(g)} \left(-\frac{\lambda_{2k}}{2k} C_{k,k}^{(2k)} \right) \Sigma_{\phi^k \phi^k}^{(g)} \left(-\frac{\lambda_{2k}}{2k} C_{k,k}^{(2k)} \right) \Sigma_{\phi^k \phi^k}^{(g)} + \dots, \end{aligned} \quad (\text{A10})$$

we get the correct contributions to EE as

$$S_{\lambda_{2k}}|_{\phi^k \phi^k} = -\frac{V_{d-1}}{12} \int \frac{d^{d-1}k_{\parallel}}{(2\pi)^{d-1}} \ln \left(1 - \left(-\frac{\lambda_{2k}}{2k} C_{k,k}^{(2k)} \right) \Sigma_{\phi^k \phi^k}^{(g)} \right). \quad (\text{A11})$$

This is the result of Equation (10). In the 2PI formalism, the result is interpreted that only the 1-loop diagram provides a single twist contributions of propagators, and all the other diagrams cancel each other. In the above discussions, we did not separate diagrams into 1-loop and others but instead used the very basic relation of Equation (A6). Then, using the property of the \mathbb{Z}_M redundancy, the logarithmic factor for the 1-loop diagram naturally appears.

The above discussion can be straightforwardly generalized to more general composite operators with operator mixings. When we have a set of operators $\{\mathcal{O}_a\}$ by opening vertices, we consider g-1PI self-energies $\Sigma_{\mathcal{O}_a \mathcal{O}_b}^{(g)}$ and a matrix generalization of the nodal structure of $(\lambda_n/n) \times C_{ab}^{(n)}$. It is also straightforward when the fundamental fields are mixed with other operators; it is sufficient to consider $\hat{\Sigma}^{(g)} \hat{G}_0$ in the formulation. As a result, we arrive at the unified form of Equation (32).

References

- Calabrese, P.; Cardy, J.L. Entanglement entropy and quantum field theory. *J. Stat. Mech.* **2004**, *0406*, P06002. [[CrossRef](#)]
- Calabrese, P.; Cardy, J. Entanglement entropy and conformal field theory. *J. Phys. A* **2009**, *42*, 504005. [[CrossRef](#)]
- Ruggiero, P.; Tonni, E.; Calabrese, P. Entanglement entropy of two disjoint intervals and the recursion formula for conformal blocks. *J. Stat. Mech.* **2018**, *1811*, 113101. [[CrossRef](#)]
- Hung, L.Y.; Myers, R.C.; Smolkin, M. Twist operators in higher dimensions. *J. High Energy Phys.* **2014**, *10*, 178. [[CrossRef](#)]
- Casini, H.; Huerta, M. Entanglement entropy for the n-sphere. *Phys. Lett. B* **2010**, *694*, 167–171. [[CrossRef](#)]
- Rosenhaus, V.; Smolkin, M. Entanglement Entropy for Relevant and Geometric Perturbations. *J. High Energy Phys.* **2015**, *2*, 15. [[CrossRef](#)]
- Rosenhaus, V.; Smolkin, M. Entanglement Entropy: A Perturbative Calculation. *J. High Energy Phys.* **2014**, *12*, 179. [[CrossRef](#)]
- Rosenhaus, V.; Smolkin, M. Entanglement entropy, planar surfaces, and spectral functions. *J. High Energy Phys.* **2014**, *9*, 119. [[CrossRef](#)]
- Ryu, S.; Takayanagi, T. Holographic derivation of entanglement entropy from AdS/CFT. *Phys. Rev. Lett.* **2006**, *96*, 181602. [[CrossRef](#)] [[PubMed](#)]

10. Ryu, S.; Takayanagi, T. Aspects of Holographic Entanglement Entropy. *J. High Energy Phys.* **2006**, *8*, 045. [[CrossRef](#)]
11. Hubeny, V.E.; Rangamani, M.; Takayanagi, T. A Covariant holographic entanglement entropy proposal. *J. High Energy Phys.* **2007**, *07*, 062. [[CrossRef](#)]
12. Nishioka, T.; Ryu, S.; Takayanagi, T. Holographic Entanglement Entropy: An Overview. *J. Phys. A* **2009**, *42*, 504008. [[CrossRef](#)]
13. Nishioka, T. Entanglement entropy: Holography and renormalization group. *Rev. Mod. Phys.* **2018**, *90*, 035007. [[CrossRef](#)]
14. Casini, H.; Huerta, M. Entanglement entropy in free quantum field theory. *J. Phys. A Math. Theor.* **2009**, *42*, 504007. [[CrossRef](#)]
15. Botero, A.; Reznik, B. Spatial structures and localization of vacuum entanglement in the linear harmonic chain. *Phys. Rev. A* **2004**, *70*, 052329. [[CrossRef](#)]
16. Katsinis, D.; Pastras, G. An Inverse Mass Expansion for Entanglement Entropy in Free Massive Scalar Field Theory. *Eur. Phys. J. C* **2018**, *78*, 282. [[CrossRef](#)]
17. Bianchi, E.; Satz, A. Entropy of a subalgebra of observables and the geometric entanglement entropy. *Phys. Rev. D* **2019**, *99*, 085001. [[CrossRef](#)]
18. Lewkowycz, A.; Myers, R.C.; Smolkin, M. Observations on entanglement entropy in massive QFT's. *J. High Energy Phys.* **2013**, *4*, 17. [[CrossRef](#)]
19. Herzog, C.P.; Nishioka, T. Entanglement Entropy of a Massive Fermion on a Torus. *J. High Energy Phys.* **2013**, *3*, 77. [[CrossRef](#)]
20. Donnelly, W.; Timmerman, S.; Valdés-Meller, N. Entanglement entropy and the large N expansion of two-dimensional Yang-Mills theory. *J. High Energy Phys.* **2020**, *4*, 182. [[CrossRef](#)]
21. Jafferis, D.L.; Klebanov, I.R.; Pufu, S.S.; Safdi, B.R. Towards the F-Theorem: $N = 2$ Field Theories on the Three-Sphere. *J. High Energy Phys.* **2011**, *06*, 102. [[CrossRef](#)]
22. Pufu, S.S. The F-Theorem and F-Maximization. *J. Phys. A* **2017**, *50*, 443008. [[CrossRef](#)]
23. Nishioka, T.; Yaakov, I. Supersymmetric Renyi Entropy. *J. High Energy Phys.* **2013**, *10*, 155. [[CrossRef](#)]
24. Hertzberg, M.P. Entanglement Entropy in Scalar Field Theory. *J. Phys. A* **2013**, *46*, 015402. [[CrossRef](#)]
25. Chen, Y.; Hackl, L.; Kunjwal, R.; Moradi, H.; Yazdi, Y.K.; Zilhão, M. Towards spacetime entanglement entropy for interacting theories. *J. High Energy Phys.* **2020**, *11*, 114. [[CrossRef](#)]
26. Metlitski, M.A.; Fuertes, C.A.; Sachdev, S. Entanglement entropy in the $O(N)$ model. *Phys. Rev. B* **2009**, *80*, 115122. [[CrossRef](#)]
27. Akers, C.; Ben-Ami, O.; Rosenhaus, V.; Smolkin, M.; Yankielowicz, S. Entanglement and RG in the $O(N)$ vector model. *J. High Energy Phys.* **2016**, *3*, 2. [[CrossRef](#)]
28. Cotler, J.; Mueller, M.T. Entanglement Entropy and Variational Methods: Interacting Scalar Fields. *Ann. Phys.* **2016**, *365*, 91–117. [[CrossRef](#)]
29. Fernandez-Melgarejo, J.J.; Molina-Vilaplana, J. Entanglement Entropy: Non-Gaussian States and Strong Coupling. *J. High Energy Phys.* **2021**, *2*, 106. [[CrossRef](#)]
30. Fernández-Melgarejo, J.J.; Molina-Vilaplana, J. On the Entanglement Entropy in Gaussian cMERA. *arXiv* **2021**, arXiv:2104.01551.
31. Whitsitt, S.; Witczak-Krempa, W.; Sachdev, S. Entanglement entropy of the large N Wilson-Fisher conformal field theory. *Phys. Rev. B* **2017**, *95*, 045148. [[CrossRef](#)]
32. Hampapura, H.R.; Lawrence, A.; Stanojevic, S. Phase transitions in the Rényi entropies of a $2 + 1D$ large- N interacting vector model. *Phys. Rev. B* **2019**, *100*, 134412. [[CrossRef](#)]
33. Wang, L.; Troyer, M. Renyi Entanglement Entropy of Interacting Fermions Calculated Using the Continuous-Time Quantum Monte Carlo Method. *Phys. Rev. Lett.* **2014**, *113*, 110401. [[CrossRef](#)]
34. Buividovich, P.V.; Polikarpov, M.I. Numerical study of entanglement entropy in $SU(2)$ lattice gauge theory. *Nucl. Phys. B* **2008**, *802*, 458–474. [[CrossRef](#)]
35. Buividovich, P.V.; Polikarpov, M.I. Entanglement entropy in gauge theories and the holographic principle for electric strings. *Phys. Lett. B* **2008**, *670*, 141–145. [[CrossRef](#)]
36. Itou, E.; Nagata, K.; Nakagawa, Y.; Nakamura, A.; Zakharov, V.I. Entanglement in Four-Dimensional $SU(3)$ Gauge Theory. *Prog. Theor. Exp. Phys.* **2016**, *2016*, 061B01. [[CrossRef](#)]
37. Rabenstein, A.; Bodendorfer, N.; Buividovich, P.; Schäfer, A. Lattice study of Rényi entanglement entropy in $SU(N_c)$ lattice Yang-Mills theory with $N_c = 2, 3, 4$. *Phys. Rev. D* **2019**, *100*, 034504. [[CrossRef](#)]
38. Wilson, K.G. Renormalization Group and Critical Phenomena. I. Renormalization Group and the Kadanoff Scaling Picture. *Phys. Rev. B* **1971**, *4*, 3174–3183. [[CrossRef](#)]
39. Wilson, K.G. Renormalization Group and Critical Phenomena. II. Phase-Space Cell Analysis of Critical Behavior. *Phys. Rev. B* **1971**, *4*, 3184–3205. [[CrossRef](#)]
40. Wilson, K.G.; Kogut, J.B. The Renormalization group and the epsilon expansion. *Phys. Rept.* **1974**, *12*, 75–199. [[CrossRef](#)]
41. Polchinski, J. Renormalization and Effective Lagrangians. *Nucl. Phys. B* **1984**, *231*, 269–295. [[CrossRef](#)]
42. Iso, S.; Mori, T.; Sakai, K. Entanglement entropy in scalar field theory and \mathbb{Z}_M gauge theory on Feynman diagrams. *Phys. Rev. D* **2021**, *103*, 105010. [[CrossRef](#)]
43. Iso, S.; Mori, T.; Sakai, K. Non-Gaussianity of entanglement entropy and correlations of composite operators. *Phys. Rev. D* **2021**, *103*, 125019. [[CrossRef](#)]
44. Yao, H.; Qi, X.L. Entanglement Entropy and Entanglement Spectrum of the Kitaev Model. *Phys. Rev. Lett.* **2010**, *105*, 080501. [[CrossRef](#)]
45. De Boer, J.; Järvelä, J.; Keski-Vakkuri, E. Aspects of capacity of entanglement. *Phys. Rev. D* **2019**, *99*, 066012. [[CrossRef](#)]

46. Nishioka, T.; Takayanagi, T. AdS bubbles, entropy and closed string tachyons. *J. High Energy Phys.* **2007**, *2007*, 090. [[CrossRef](#)]
47. He, S.; Numasawa, T.; Takayanagi, T.; Watanabe, K. Notes on Entanglement Entropy in String Theory. *J. High Energy Phys.* **2015**, *5*, 106. [[CrossRef](#)]
48. Wetterich, C. Exact evolution equation for the effective potential. *Phys. Lett. B* **1993**, *301*, 90–94. [[CrossRef](#)]
49. Morris, T.R. The Exact renormalization group and approximate solutions. *Int. J. Mod. Phys. A* **1994**, *9*, 2411–2450. [[CrossRef](#)]
50. Iso, S.; Mori, T.; Sakai, K. KEK Theory Center, High Energy Accelerator Research Organization (KEK), Tsukuba, Ibaraki, Japan; 2021. Manuscript in Preparation
51. Fernandez-Melgarejo, J.J.; Molina-Vilaplana, J. Non-Gaussian Entanglement Renormalization for Quantum Fields. *J. High Energy Phys.* **2020**, *7*, 149. [[CrossRef](#)]
52. Eisert, J.; Cramer, M.; Plenio, M.B. Area laws for the entanglement entropy—A review. *Rev. Mod. Phys.* **2010**, *82*, 277–306. [[CrossRef](#)]
53. Kawabata, K.; Nishioka, T.; Okuyama, Y.; Watanabe, K. Probing Hawking radiation through capacity of entanglement. *J. High Energy Phys.* **2021**, *05*, 062. [[CrossRef](#)]
54. Okuyama, K. Capacity of entanglement in random pure state. *arXiv* **2021**, arXiv:2103.08909.
55. Kawabata, K.; Nishioka, T.; Okuyama, Y.; Watanabe, K. Replica wormholes and capacity of entanglement. *arXiv* **2021**, arXiv:2105.08396.
56. Hastings, M.B. An area law for one-dimensional quantum systems. *J. Stat. Mech.* **2007**, *0708*, P08024. [[CrossRef](#)]
57. Bueno, P.; Casini, H.; Witczak-Krempa, W. Generalizing the entanglement entropy of singular regions in conformal field theories. *J. High Energy Phys.* **2019**, *08*, 069. [[CrossRef](#)]
58. Ogawa, N.; Takayanagi, T.; Ugajin, T. Holographic Fermi Surfaces and Entanglement Entropy. *J. High Energy Phys.* **2012**, *1*, 125. [[CrossRef](#)]
59. Shiba, N.; Takayanagi, T. Volume Law for the Entanglement Entropy in Non-local QFTs. *J. High Energy Phys.* **2014**, *2*, 033. [[CrossRef](#)]
60. Vitagliano, G.; Riera, A.; Latorre, J.I. Violation of area-law scaling for the entanglement entropy in spin 1/2 chains. *New J. Phys.* **2010**, *12*, 113049. [[CrossRef](#)]
61. Ramírez, G.; Rodríguez-Laguna, J.; Sierra, G. From conformal to volume law for the entanglement entropy in exponentially deformed critical spin 1/2 chains. *J. Stat. Mech. Theory Exp.* **2014**, *2014*, P10004. [[CrossRef](#)]
62. He, T.; Magan, J.M.; Vandoren, S. Entanglement Entropy in Lifshitz Theories. *SciPost Phys.* **2017**, *3*, 34. [[CrossRef](#)]
63. Mohammadi Mozaffar, M.R.; Mollabashi, A. Entanglement in Lifshitz-type Quantum Field Theories. *J. High Energy Phys.* **2017**, *7*, 120. [[CrossRef](#)]
64. Gentle, S.A.; Vandoren, S. Lifshitz entanglement entropy from holographic cMERA. *J. High Energy Phys.* **2018**, *7*, 013. [[CrossRef](#)]